1521-0111/90/6/726–737$25.00
MOLECULAR PHARMACOLOGY

http://dx.doi.org/10.1124/mol.116.106112
Mol Pharmacol 90:726–737, December 2016

Discovery and Characterization of Novel GPR39 Agonists Allosterically Modulated by Zinc[S]

Seiji Sato, Xi-Ping Huang, Wesley K. Kroeze, and Bryan L. Roth

Department of Pharmacology (S.S., X.-P.H., W.K.K., B.L.R.) and National Institute of Mental Health Psychoactive Drug Screening Program (X.-P.H., B.L.R.), School of Medicine, University of North Carolina, Chapel Hill, North Carolina

Received July 13, 2016; accepted September 15, 2016

ABSTRACT

In this study, we identified two previously described kinase inhibitors—3-(4-chloro-2-fluorobenzyl)-2-methyl-*N*-(3-methyl-1H-pyrazol-5-yl)-8-(morpholinomethyl)imidazo[1,2-b]pyridazin-6-amine (LY2784544) and 1H-benzimidazole-4-carboxylic acid, 2-methyl-1-[[2-methyl-3-(trifluoromethyl)phenyl]methyl]-6-(4-morpholinyl)- (GSK2636771)—as novel GPR39 agonists by unbiased small-molecule-based screening using a β-arrestin recruitment screening approach (PRESTO-Tango). We characterized the signaling of LY2784544 and GSK2636771 and compared their signaling patterns with a previously described "GPR39-selective" agonist *N*-[3-chloro-4-[[[2-(methylamino)-6-(2-pyridinyl)-4-pyrimidinyl]amino]methyl]phenyl]methanesulfonamide (GPR39-C3) at both canonical and noncanonical signaling pathways. Unexpectedly, all three compounds displayed probe-dependent and pathway-dependent allosteric modulation by concentrations of zinc reported to be physiologic. LY2784544 and GS2636771 at GPR39 in the presence of zinc were generally as potent or more potent than their reported activities against kinases in whole-cell assays. These findings reveal an unexpected role of zinc as an allosteric potentiator of small-molecule-induced activation of GPR39 and expand the list of potential kinase off-targets to include understudied G protein–coupled receptors.

Introduction

G protein–coupled receptors (GPCRs) transduce extracellular stimuli into intracellular signals, have crucial roles in virtually all of human physiology, and are the targets for about one-third of currently marketed drugs (Overington et al., 2006; Rask-Andersen et al., 2014). When agonists bind to GPCRs, signals are transduced into cells via a number of Gα proteins, or β-arrestins, and other interacting proteins. In the human genome, there are about 350 nonolfactory GPCRs, of which about 100 are still orphans, i.e., their endogenous ligands are yet unknown (Vassilatis et al., 2003; Fredriksson and Schiöth, 2005; Bjarnadóttir et al., 2006; Regard et al., 2008; Komatsu et al., 2014; Roth and Kroeze, 2015), or alternatively, they are very poorly annotated with respect to ligands, whether endogenous or surrogate. In the current study, we report on the discovery of novel surrogate ligands for GPR39, previously described as a zinc receptor (Holst et al., 2007).

GPR39 is a member of the ghrelin peptide receptor family. Although the ligands of the nonorphan receptors in this family are all peptides [ghrelin, growth hormone secretagogue receptor (Kojima et al., 1999); neurotensin, NTSR1 and NTSR2 (Tanaka et al., 1990; Vita et al., 1998); motilin, MLNR (Feighner et al., 1999); neuromedin U, NMUR1 and NMUR2 (Kojima et al., 2000; Bhattacharyya et al., 2004)], GPR39 has been reported to be a Zn^{2+} metal ion–sensing receptor (Holst et al., 2007). Other divalent metal ions, such as Ni^{2+}, Cd^{2+}, Cr^{2+}, and Fe^{2+}, have also been reported to activate GPR39 (Holst et al., 2007; Huang et al., 2015). GPR39 is widely expressed in several organs, including the gastrointestinal tract, pancreas, thyroid, brain, and others (Popovics and Stewart, 2011).

GPR39 has been reported to be associated with type 2 diabetes (Holst et al., 2009; Verhulst et al., 2011) and depression (Młyniec and Nowak, 2015; Młyniec et al., 2015a,b,c). GPR39 has been found to be expressed in mouse intestinal fibroblast-like cells (Zeng et al., 2012), human colon adenocarcinoma HT-29 cells (Yasuda et al., 2007; Cohen et al., 2012, 2014), rat colon BRIN-BD11 cells (Moran et al., 2016), and mouse pancreatic epithelial NIT-1 cells (Fjellström et al., 2015). All of these cell types respond to Zn^{2+} via various signal transduction pathways. Early studies reported the peptide obestatin to be a

This work was supported by the National Institutes of Health [Grant U01-MH104974].
dx.doi.org/10.1124/mol.116.106112.
[S] This article has supplemental material available at molpharm.aspetjournals.org.

ABBREVIATIONS: AZ1395, 3,4-bis-(2-imidazol-1-ylethoxy)-benzonitrile; AZ4237, 6-[(4-chlorophenyl)methyl]-7-hydroxy-5-methyl-pyrazolo[1,5-a]pyrimidine-3-carboxylic acid; AZ7914, 6-(3-chloro-2-fluoro-benzoyl)-2-(2-methylthiazol-4-yl)-3,5,7,8-tetrahydropyrido-[4,3-d]pyrimidin-4-one; DMEM, Dulbecco's modified Eagle's medium; FBS, fetal bovine serum; GPCR, G protein–coupled receptor; GPR39-C3, *N*-[3-chloro-4-[[[2-(methylamino)-6-(2-pyridinyl)-4- pyrimidinyl]amino]methyl]phenyl]methanesulfonamide; GSK2636771, 1H-benzimidazole-4-carboxylic acid, 2-methyl-1-[[2-methyl-3-(trifluoromethyl)phenyl]methyl]-6-(4-morpholinyl)-; HBSS, Hanks' balanced salt solution; HEK293T, human embryonic kidney 293T; HTLA, HEK293-derived cell line containing stable integrations of a tetracycline transactivator–dependent luciferase reporter and a β-arrestin2–tobacco etch virus fusion gene; IBMX, 3-isobutyl-1-methylxanthine; LY2784544, 3-(4-chloro-2-fluorobenzyl)-2-methyl-*N*-(3-methyl-1H-pyrazol-5-yl)-8-(morpholinomethyl)imidazo[1,2-b]pyridazin-6-amine; PAM, positive allosteric modulator; PBS, phosphate-buffered saline; PTEN, phosphatase and tensin homolog deleted from chromosome 10; RLU, relative luminescence units.

GPR39 agonist (Zhang et al., 2005), but subsequent work failed to reproduce these results (Lauwers et al., 2006; Holst et al., 2007; Zhang et al., 2007). Zn^{2+} stimulates signaling via the Gq and β-arrestin pathways, as well as the Gs pathway (Holst et al., 2007). Recently, three groups reported small-molecule agonists for GPR39 (Boehm et al., 2013; Peukert et al., 2014; Fjellström et al., 2015). However, the signaling pathways induced by these agonists, and their relationship to Zn^{2+} concentrations, remain to be elucidated. Additionally, the physiologic significance of each GPR39 signaling pathway remains unclear. Here, we provide an approach for discovering new GPR39 agonists useful for illuminating GPR39 signaling pathways. We exemplify two compounds and elucidate how their signaling is allosterically modulated by Zn^{2+}.

Materials and Methods

Compounds. The following libraries were screened in quadruplicate using a modified TANGO β-arrestin recruitment assay (Barnea et al., 2008; Kroeze et al., 2015) for activity at GPR39: NCC-1 (446 compounds; National Clinical Collection), NIMH X-901 (271 compounds; National Institute of Health Clinical Collection, Bethesda, MD), Prestwick (1120 compounds; Illkirch, France), Tocris (1280 compounds; Bristol, UK), Selleckchem (1836 compounds; Munich, Germany), and Spectrum (2400 compounds; MicroSource, Gaylordsville, CT) at a drug concentration of 10 μM to which transfected cells was exposed, following the previously published method (Kroeze et al., 2015). Daughter libraries were prepared and kept at −20°C until use. 3-(4-Chloro-2-fluorobenzyl)-2-methyl-*N*-(3-methyl-1H-pyrazol-5-yl)-8-(morpholinomethyl)imidazo [1,2-b]pyridazin-6-amine (LY2784544), 1H-benzimidazole-4-carboxylic acid, 2-methyl-1-[[2-methyl-3-(trifluoromethyl)phenyl]methyl]-6-(4-morpholinyl)-(GSK2636771), *N*-[3-chloro-4-[[[2-(methylamino)-6-(2-pyridinyl)-4- pyrimidinyl]amino]methyl]phenyl]methanesulfonamide (GPR39-C3), and obestatin were obtained from Selleckchem, MedChem Express (Monmouth Junction, NJ), Xcessbio (San Diego, CA), and Sigma-Aldrich (St. Louis, MO), respectively.

Site-Directed Mutagenesis. The His17Ala/His19Ala mutation in GPR39 was introduced using the GPR39-TANGO construct (Kroeze et al., 2015) as a template, PrimeSTAR Max (TAKARA Clontech, Mountain View, CA) as the polymerase, and the following primers: 39T-H17AH19A_S: 5′- GACGCTAGCGCTGTGCCGGAGTTTGAAG-TGGC -3′, 39T-H17AH19A_A: 5′- CACAGCGCTAGCGTCAA-TAATCTGGCTACAGT-3′. Mutations were confirmed by sequencing (Eton Bioscience Inc., Research Triangle Park, NC). For assessment of G protein–mediated signaling, GPR39-TANGO constructs were "de-TANGO-ized" by introduction of a stop codon

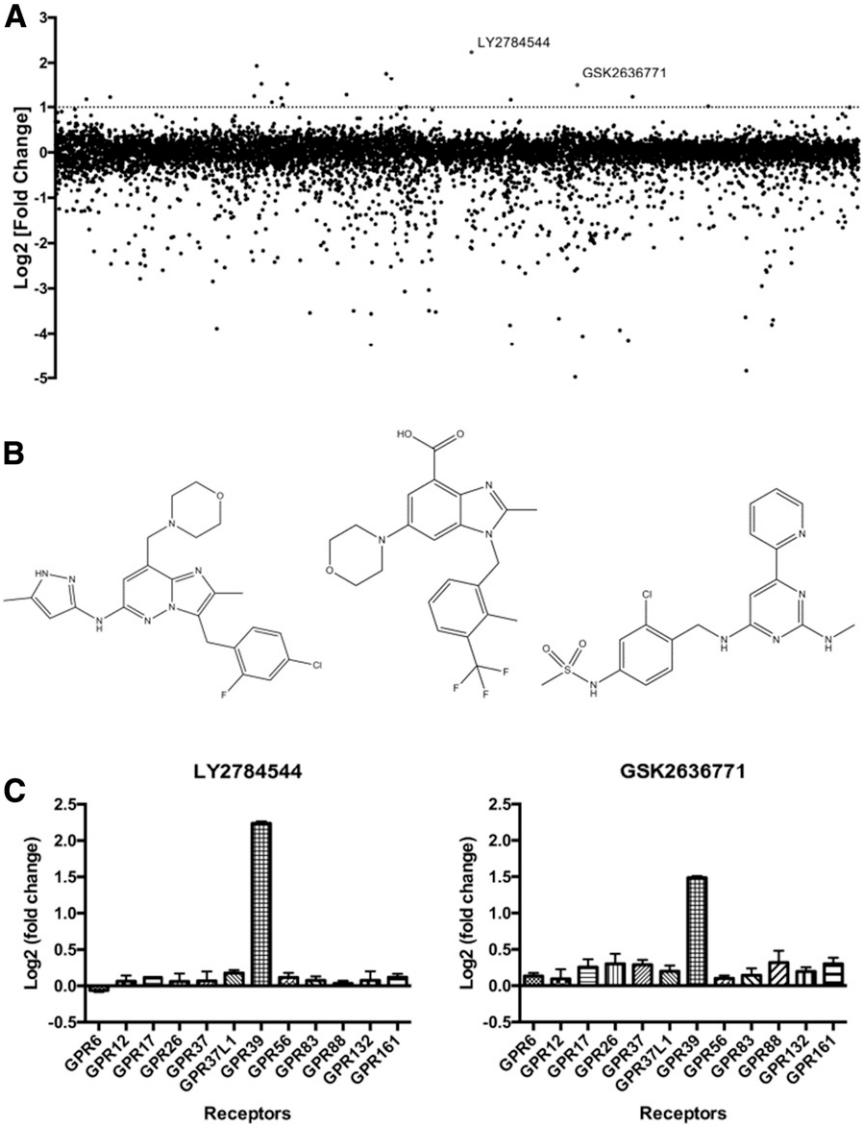

Fig. 1. Summary of drug screening at GPR39 using the TANGO β-arrestin recruitment assay. (A) Screening was carried out in quadruplicate at 10 μM drug concentration. After excluding promiscuous activators, LY2784544 and GSK2636771 were identified as GPR39-selective agonists for the β-arrestin pathway (B and C). (B) Structures of LY2784544 (middle) and GSK2636771 (right) and a previously described GPR39 (left) agonist, GPR39-C3. (C) Activities of LY2784544 and GSK2636771 at GPR39 and 11 additional understudied GPCRs.

immediately following the GPR39 open reading frame using the primers TangoUniStopCleanF (5′-GACGCACCTAGCTCGAGTCTAGAGGGCCCG-3′) and TangoUniStopCleanR (5′-CTCGAGCTAGGTGCGTCCACCGGTATCGAT-3′), and confirmed by sequencing.

TANGO Assay. HTLA cells [a human embryonic kidney 293 (HEK293) cell line stably expressing a tetracycline transactivator–dependent luciferase reporter and a β-arrestin2–tobacco etch virus fusion gene] were a gift from the laboratory of R. Axel (Columbia University, New York, NY) and were maintained in Dulbecco's modified Eagle's medium (DMEM) supplemented with 10% fetal bovine serum (FBS), 100 U/ml penicillin, 100 μg/ml streptomycin, 2 μg/ml puromycin, and 100 μg/ml hygromycin B in a humidified atmosphere at 37°C in 5% CO_2. TANGO β-arrestin recruitment assays were carried out as described by Kroeze et al. (2015). All experiments were performed in quadruplicate. Results expressed as relative luminescence units (RLU) were exported into Excel spreadsheets (Microsoft, Redmond, WA), and analyses were done using GraphPad Prism (GraphPad Software, La Jolla, CA). To calculate fold change, wells without compounds and without Zn^{2+} were used as "basal"; results were finally expressed as log2-fold change.

PRESTO-Tango GPCR-ome Profiling. The PRESTO-Tango GPCR-ome assay was performed as previously described (Kroeze et al., 2015). HTLA cells were cultured in poly-L-Lys–coated 384-well white clear-bottom cell culture plates (Greiner, Monroe, NC) in DMEM supplemented with 10% dialyzed FBS at a density of 10,000 cells/well in a total volume of 50 μl 1 day before transfection. The next day, 40 ng/well DNA was transfected into each well using the calcium phosphate precipitation method. The following day, the medium was aspirated from the plate and replaced with 50 μl/well fresh DMEM containing 1% dialyzed FBS and 100 μM $ZnCl_2$, with or without 1 μM compound, and incubated overnight. DRD2 and 1 μM quinpirole were set on every plate as a positive control for this assay. The detection step was performed using the method described by Kroeze et al. (2015). All experiments were done in quadruplicate. Results expressed as RLU were exported into Excel spreadsheets, and analyses were done using GraphPad Prism. The mean fold change for each receptor was calculated as (mean RLU with ligand/mean RLU without ligand).

Inositol Phosphate Accumulation Assay. Inositol phosphate accumulation assays were performed as in previous reports (https://pdspdb.unc.edu/pdspWeb/content/PDSP%20Protocols%20II%202013-03-28.pdf; Storjohann et al., 2008). HEK293T cells were maintained in DMEM supplemented with 10% FBS, 100 U/ml penicillin, and 100 μg/ml streptomycin. Cells were transfected with 20 μg of receptor DNA per 15-cm cell-culture dish and incubated overnight at 37°C in a humidified 5% CO_2 incubator. The next day, 30,000 cells/well were seeded into poly-L-lysine–coated 96-well plates in 100 μl/well DMEM supplemented with 10% dialyzed FBS, 100 U/ml penicillin, and 100 μg/ml streptomycin. After attaching to the plate, cells were incubated for 16 hours as described earlier in inositol-free DMEM (United States Biological, Salem, MA) containing 10% dialyzed FBS and 1 μCi/well of myo-[^{3}H]inositol (PerkinElmer, Waltham, MA). On the following day, cells were washed with 100 μl of drug buffer [1× Hanks' balanced salt solution (HBSS), 24 mM $NaHCO_3$, 11 mM glucose, and 15 mM LiCl, pH 7.4] and treated with 100 μl of drug buffer containing drug and 0.3% bovine serum albumin (Sigma-Aldrich) in quadruplicate for 1 hour at 37°C in a 5% CO_2 incubator. After treatment, drug solution was removed by aspiration, and 40 μl of 50 mM formic acid was added to lyse cells for 30 minutes at 4°C. After cell lysis, 20 μl of the acid extract was transferred to each well of a polyethylene terephthalate 96-well sample plate (1450-401; PerkinElmer) and mixed with 75 μl of PerkinElmer RNA Binding YSi SPA Beads (RPNQ0013) at a concentration of 0.2 mg beads/well and incubated for 30 minutes at room temperature. Bead/lysate mixtures were then counted with a Microbeta Trilux counter (Perkin-Elmer, Boston, MA). Data were exported into Excel spreadsheets and analyzed using GraphPad Prism.

cAMP Accumulation Assay. Receptor-mediated Gs pathway signaling was measured using a split-luciferase receptor assay (GloSensor cAMP assay; Promega, Madison, WI). In brief, HEK293T cells were transiently cotransfected with receptor DNA and the GloSensor cAMP reporter plasmid (GloSensor 7A). The following day, transfected cells were plated into poly-L-lysine–coated 384-well white clear-bottom cell culture plates in DMEM supplemented with 1% dialyzed FBS (Omega Scientific, Tarzana, CA), 100 U/ml penicillin, and 100 μg/ml streptomycin at a density of 15,000 cells/well in a total volume of 40 μl. The next day, culture medium was removed by aspiration, and cells were incubated with 20 μl of 4 mM luciferin (GoldBio, St. Louis, MO) prepared in drug buffer (20 mM HEPES, 1× HBSS, and 0.3% bovine serum albumin, pH 7.4) for 30 minutes at 37°C. Next, cells were incubated with 10 μl of a 3× concentration of drug at room temperature for 15 minutes. Following drug treatment, cells were incubated with 10 μl of a 4× concentration of $ZnCl_2$ solution in drug buffer, or drug buffer alone, for 15 minutes at room temperature. Luminescence was then counted using a Microbeta Trilux luminescence counter (PerkinElmer). All experiments were performed in quadruplicate and exported into Excel spreadsheets, which were then analyzed using GraphPad Prism. To calculate fold change, wells without compounds and without Zn^{2+} were used as "basal."

Cell Enzyme-Linked Immunosorbent Assay. To confirm cell surface expression of the FLAG-tagged GPR39 and its mutants, immunohistochemistry was done using cells plated into 384-well plates, as described earlier, at 10,000 cells/well. Cells were fixed with 20 μl/well 4% paraformaldehyde for 10 minutes at room temperature. After fixation, cells were washed twice with 40 μl/well of phosphate-buffered saline (PBS) at pH 7.4. Blocking was done with 20 μl/well 5% normal goat serum in PBS for 30 minutes at room temperature. After

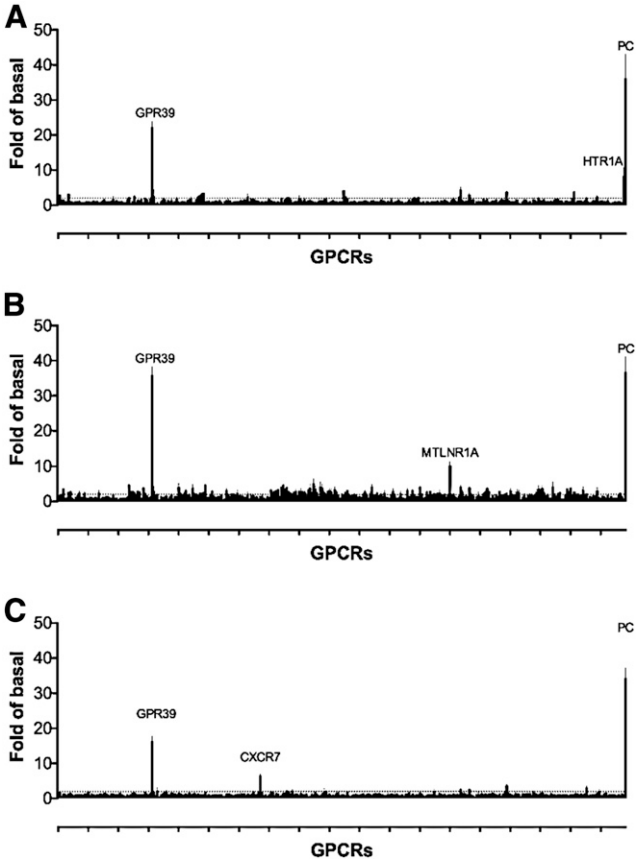

Fig. 2. GPCR-ome (PRESTO-Tango) analysis of three compounds: GPR39-C3 (A), LY2784544 (B), and GSK2636771 (C). These assays were performed using 1 μM concentrations of each compound with 100 μM $ZnCl_2$. The results are the mean ± S.E.M. of quadruplicate determinations. The right-most bar (PC) represents the positive control, which was the DRD2 dopamine receptor stimulated with 1 micromolar of the agonist quinpirole.

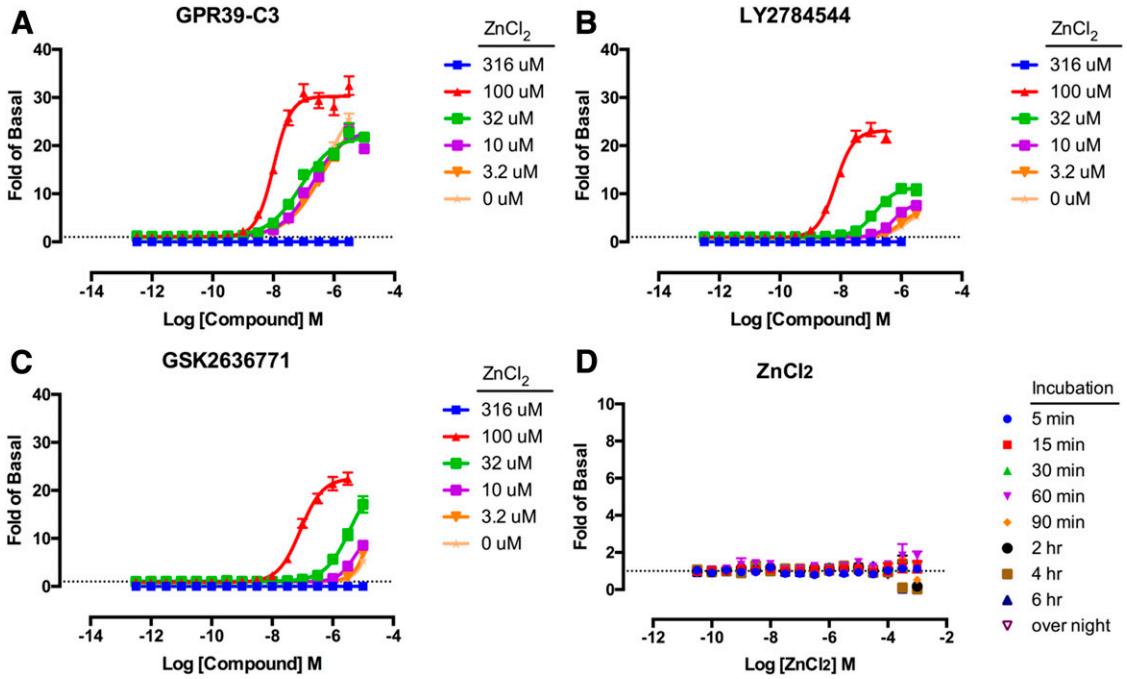

Fig. 3. Concentration-dependent and GPR39-dependent β-arrestin recruitment as measured by the TANGO assay in response to GPR39-C3 (A), LY2784544 (B), or GSK2636771 (C) in the presence of various concentrations of Zn^{2+}. (D) Zn^{2+} stimulations were carried out at several different incubation times with Zn^{2+} from 5 minutes to 6 hours, followed by washing and incubation with fresh medium or overnight incubation with Zn^{2+}. The results are expressed as the fold of basal and are the mean ± S.E.M. of three independent experiments, each performed in quadruplicate.

blocking, 20 μl/well anti-FLAG–horseradish peroxidase–conjugated antibody (Sigma-Aldrich) diluted 1/10,000 was added and incubated for 1 hour at room temperature. This was followed by two washes with 80 μl/well PBS. Then, 20 μl/well SuperSignal Enzyme-Linked Immunosorbent Assay Pico Substrate (Sigma-Aldrich) was added, and luminescence was counted using a MicroBeta Trilux luminescence counter. Expression of mutants was normalized by using expression of wild-type receptors as 100% and untransfected cells as 0%. As previously stated, all experiments were done in quadruplicate.

Fluorescent Imaging Plate Reader Assay. HT-29 (ATCC) and PC-3 (obtained from Kim Laboratory, The Lineberger Comprehensive Cancer Center, University of North Carolina, Chapel Hill) were maintained in 10% FBS, McCoy's 5A medium (Gibco, Thermo Fisher Scientific, Waltham, MA) plus 10% FBS, and DMEM plus 10% FBS, respectively. The cells were seeded into poly-L-Lys–coated 384-well black clear-bottom cell culture plates in each medium supplemented with 10% dialyzed fetal bovine serum at a density of 10,000 cells/well in a total volume of 50 μl 1 day before assay. The following day, medium was discarded, and cells were loaded with 20 μl/well of 1× Fluo-4 Direct Calcium dye (20 mM HEPES, 1× HBSS, 2.5 mM probenecid, pH 7.40) (Thermo Fisher Scientific). Plates were incubated for 60 minutes at 37°C. The fluorescent imaging plate reader was programmed to take 10 readings (1 read per second) first as a baseline before addition of 10 μl of 3× drug solutions. The fluorescence intensity was recorded for 2 minutes after drug addition.

Results

Discovery of Novel GPR39 Agonists. The TANGO β-arrestin recruitment assay was used to screen several compound libraries (*Materials and Methods*), totaling

TABLE 1
Pharmacological parameters of results shown in Fig. 3, A–C
Top and bottom are expressed as fold of basal, and log EC_{50} is expressed as logged EC_{50} (M).

	$ZnCl_2$					
	316 μM (N = 3)	100 μM (N = 8)	31.6 μM (N = 3)	10 μM (N = 3)	3.2 μM (N = 3)	0 μM (N = 8)
GPR39-C3						
Top	0.04 ± 0.00	30.27 ± 0.57	22.03 ± 0.71	23.23 ± 0.88	26.81 ± 1.92	33.25 ± 2.31
Bottom	0.01 ± 0.00	1.09 ± 0.36	0.98 ± 0.21	0.99 ± 0.20	0.95 ± 0.19	1.00 ± 0.16
Log EC_{50}	−8.63 ± 0.17	−7.99 ± 0.04	−7.09 ± 0.06	−6.72 ± 0.06	−6.40 ± 0.11	−6.22 ± 0.11
Hill slope	0.82 ± 0.24	1.52 ± 0.17	0.79 ± 0.07	0.83 ± 0.08	0.72 ± 0.07	0.69 ± 0.05
LY2784544						
Top	0.03 ± 0.00	23.16 ± 0.52	11.38 ± 0.45	7.99 ± 0.33	6.59 ± 0.51	7.10 ± 0.78
Bottom	0.01 ± 0.00	0.89 ± 0.25	1.02 ± 0.12	0.97 ± 0.06	0.92 ± 0.05	1.00 ± 0.03
Log EC_{50}	−8.93 ± 0.27	−8.17 ± 0.04	−6.86 ± 0.06	−6.26 ± 0.04	−6.03 ± 0.07	−5.81 ± 0.11
Hill slope	1.10 ± 0.66	1.45 ± 0.15	1.28 ± 0.17	1.61 ± 0.20	1.51 ± 0.25	1.27 ± 0.16
GSK2636771						
Top	0.03 ± 0.00	22.56 ± 0.59	22.96 ± 3.48	10.84 ± 0.99	>153.7	>73.15
Bottom	0.00 ± 0.00	0.83 ± 0.21	1.05 ± 0.16	0.99 ± 0.04	0.97 ± 0.05	1.00 ± 0.03
Log EC_{50}	−7.96 ± 0.29	−7.07 ± 0.04	−5.42 ± 0.16	−5.31 ± 0.07	>-4.07	>-4.25
Hill slope	0.64 ± 0.25	1.18 ± 0.11	1.04 ± 0.17	1.66 ± 0.21	1.50 ± 1.02	1.59 ± 0.86

approximately 5000 unique compounds, for agonist activity at GPR39 in the absence of Zn^{2+}. Approximately 20 compounds showed activities over 2-fold higher than basal (i.e., log2-fold change > 1) (Fig. 1A); after exclusion of promiscuous compounds that also activated other GPCR targets (data not shown), the JAK2 inhibitor LY2784544 and the PI3Kβ inhibitor GSK2636771 were identified as GPR39 agonists (Fig. 1A). The structures of these compounds are similar to each other, but are markedly different from the GPR39-C3 compound that has previously been reported to be an agonist at GPR39 (Fig. 1B; Peukert et al., 2014). When tested at 11 other GPCRs, neither of these compounds showed agonist activity (Fig. 1C). Additionally, we also tested obestatin, which has previously been reported to be a GPR39 agonist (Zhang et al., 2005), for activity at GPR39 and found it to be inactive (Supplemental Fig. 1A); we then tested obestatin for activity at 320 GPCRs using the PRESTO-Tango method (Kroeze et al., 2015; Manglik et al., 2016) and found it to be inactive at all targets tested (Supplemental Fig. 1B), both in the presence and absence of Zn^{2+}. Additionally, we performed a GPCR-ome analysis (Kroeze et al., 2015; Manglik et al., 2016) for all three GPR39 agonist compounds, i.e., GPR39-C3, LY2784544, and GSK2636771. At 1 μM concentrations, and in the presence of 100 μM $ZnCl_2$, each compound showed obvious activity at only one receptor in addition to GPR39: HTR1A by GPR39-C3, MTLNR1A by LY2784544, and CXCR7 by GSK2636771, respectively (Fig. 2, A–C). Thus, these compounds are highly specific agonists at GPR39. These activities were subsequently confirmed with concentration-response curves (Supplemental Fig. 2).

Allosteric Modulation of GPR39 β-Arrestin Recruitment Activity. Since Zn^{2+} had previously been reported to be an agonist at GPR39, and because it seemed unlikely that these compounds might be interacting at the zinc site, we wondered if zinc allosterically modulated the GPR39 agonist activity of small molecules. We used the previously reported GPR39

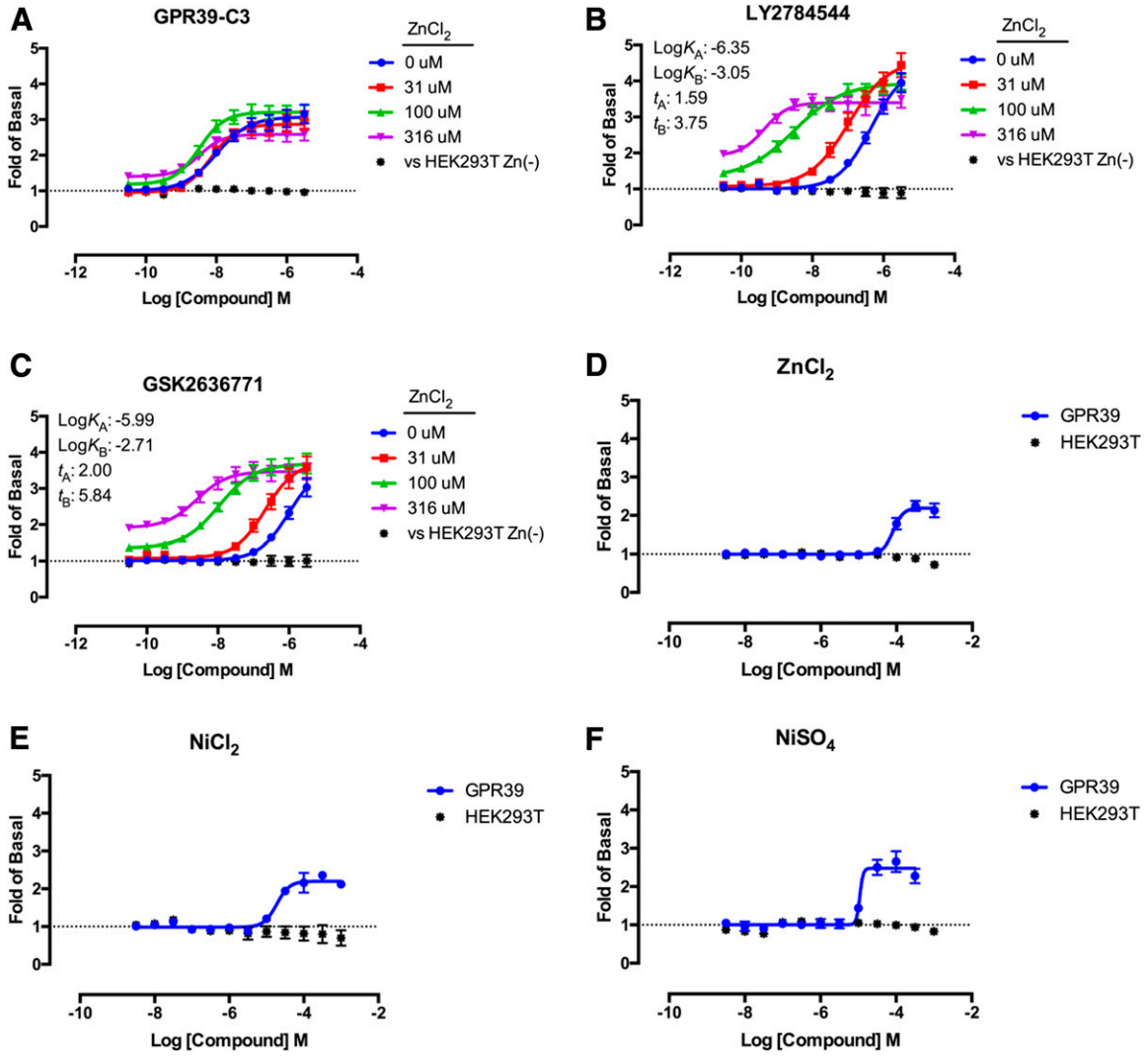

Fig. 4. Concentration-dependent and GPR39-dependent phosphatidylinositol hydrolysis (Gq pathway) in response to GPR39-C3 (A), LY2784544 (B), or GSK2636771 (C) with various concentrations of Zn^{2+}. According to an allosteric operational model, the allosteric parameters were calculated (Kenakin, 2012). τ_A is the orthosteric agonist (LY2784544 and GSK2636771) efficacy parameter. Since allosteric modulators in this study showed agonist activity, the allosteric modulator efficacy (τ_B) is therefore greater than 0. Concentration-dependent and GPR39-dependent PI hydrolysis (Gq pathway) in response to $ZnCl_2$ (D), $NiCl_2$ (E), and $NiSO_4$ (F). Black dots show response to compounds in untransfected HEK293T cells. The results are the mean ± S.E.M. of at least three independent experiments performed in quadruplicate (compounds and $ZnCl_2$) or duplicate ($NiCl_2$).

TABLE 2
Pharmacological parameters of results shown in Fig. 3, A–C
Top and bottom are expressed as fold of basal, and log EC_{50} is expressed as logged EC_{50} (M).

	$ZnCl_2$			
	316 μM (N = 4)	100 μM (N = 4)	31.6 μM (N = 4)	0 μM (N = 4)
GPR39-C3				
Top	2.59 ± 0.06	3.21 ± 0.08	2.87 ± 0.08	3.07 ± 0.10
Bottom	1.40 ± 0.09	1.18 ± 0.11	0.96 ± 0.10	1.00 ± 0.10
Log EC_{50}	−8.49 ± 0.13	−8.48 ± 0.10	−8.16 ± 0.11	−8.00 ± 0.12
Hill slope	1.29 ± 0.46	1.20 ± 0.30	1.18 ± 0.30	0.94 ± 0.23
LY2784544				
Top	3.40 ± 0.38	3.94 ± 0.30	4.57 ± 0.12	4.41 ± 0.07
Bottom	1.92 ± 0.07	1.31 ± 0.11	1.07 ± 0.22	1.00 ± 0.22
Log EC_{50}	−9.36 ± 0.14	−8.51 ± 0.14	−6.98 ± 0.16	−6.35 ± 0.19
Hill slope	1.30 ± 0.18	0.63 ± 0.17	0.79 ± 0.15	0.94 ± 0.59
GSK2636771				
Top	3.47 ± 0.09	3.68 ± 0.12	3.75 ± 0.27	3.68 ± 0.63
Bottom	1.91 ± 0.15	1.36 ± 0.12	1.08 ± 0.08	1.01 ± 0.05
Log EC_{50}	−8.60 ± 0.18	−7.97 ± 0.13	−6.67 ± 0.14	−5.99 ± 0.25
Hill slope	1.01 ± 0.38	0.86 ± 0.20	1.01 ± 0.25	1.01 ± 0.28

agonist GPR39-C3 (Peukert et al., 2014), as well as the two compounds discovered in our screens, LY2784544 and GSK2636771 (Fig. 1), at various concentrations of Zn^{2+} in the TANGO assay (Fig. 3). Zn^{2+} alone showed very little activity in this assay (Fig. 3D). However, all three compounds showed a Zn^{2+}-dependent increase in potency and efficacy up to a Zn^{2+} concentration of 100 μM (Fig. 3, A–C); at a Zn^{2+} concentration of 316 μM, no activity was seen, presumably due to the toxic effects of Zn^{2+} at such high concentrations. In an attempt to determine whether responses to Zn^{2+} could be seen with shorter exposures to its potentially toxic effects, we exposed GPR39-expressing HTLA cells to Zn^{2+} for various times, followed by a washout, and continued incubation overnight; longer exposures to higher concentrations of Zn^{2+} were apparently toxic to cells, but significant β-arrestin recruitment activity was not seen at any concentration, or with any length of exposure (Fig. 3D). The efficacy and potency values for these three compounds at various Zn^{2+} concentrations are shown in Table 1; all three compounds showed E_{max} values between 20- and 30-fold above basal at 100 μM Zn^{2+}. Interestingly, GPR39-C3 showed marked activity in the absence of Zn^{2+}, whereas LY2784544 and GSK2636771 had minimal or no activity in the absence of zinc. Taken together, the results shown in Table 1 indicate that Zn^{2+} acts as a positive allosteric modulator (PAM) of the activity of GPR39-C3 in terms of efficacy only, whereas Zn^{2+} was a PAM for the activities of LY2784544 and GSK2636771 in terms of both efficacy and potency. It should be noted that all three compounds were apparently toxic to HTLA cells at high concentrations, and therefore, data from these high concentrations were excluded from this analysis. We also tested whether LY2784544 could act as an antagonist to the GPR39-C3 response at various Zn^{2+} concentrations, and found that LY2784544 did not antagonize the GPR39-C3 response (Supplemental Fig. 3). Together, our results suggest that Zn^{2+} stabilizes a conformation of GPR39 that can be further activated to recruit β-arrestin by LY2784544. In addition, Ni^{2+} was also shown to be an agonist of GPR39 in β-arrestin recruitment activity (Fig. 4), as had previously been reported using a bioluminescence resonance energy transfer assay (Holst et al., 2007).

Allosteric Modulation of GPR39 Gq-Mediated Signaling. We also measured GPR39-mediated Gq pathway signaling using a phosphatidylinositol hydrolysis assay. As can be seen in Fig. 4, A–C, all three tested compounds stimulated Gq signaling. The Zn^{2+} dependence of responses to LY2784544 (Fig. 4B) and GSK2636771 (Fig. 4C) was much greater than that of GPR39-C3 (Fig. 4A), with leftward shifts of more than 1000-fold compared with less than 10-fold for GPR39-C3. At the higher Zn^{2+} concentrations, all three compounds were much more potent with respect to Gq signaling (Fig. 4, A–C) than they were in β-arrestin recruitment (Fig. 3), showing EC_{50} values in the low nanomolar range (Table 2). The allosteric parameters were calculated according to the Black-Leff Ehlert model (Kenakin, 2012). The allosteric modulator efficacy values (τ_B) were greater than 0, indicating that Zn^{2+} is a PAM agonist (Fig. 4, B and C). All three compounds showed a maximal efficacy of 3- to 4-fold over basal (Table 2). The maximal efficacy of all three compounds at GPR39 in Gq signaling was not affected by Zn^{2+} concentration (Fig. 4, A–C; Table 2), although Zn^{2+} and Ni^{2+} stimulated GPR39-mediated Gq signaling on their own (Fig. 4, D–F; Table 3). Interestingly, the potency of Ni^{2+} was slightly higher than that of Zn^{2+}. All of these divalent metal ions showed steep Hill slopes (>2.5) (Table 3), which we interpret to mean that divalent metal ions can act as their own PAMs at GPR39. The concentrations at which Zn^{2+} was active in this assay, i.e., in the high micromolar range, were comparable to those seen in vivo (Foster et al., 1993; Caroli et al., 1994; Lu et al., 2012). Zinc has been estimated at 200–320 μM in vivo in hippocampus mossy fibers (GPR39 is enriched in the hippocampus) (Frederickson et al., 1983) and at levels >100 μM during synaptic transmission (Assaf and Chung, 1984). The concentrations we used in our experiments (3.4–340 μM) are in this range. Taken together, these

TABLE 3
Pharmacological parameters of results shown in Fig. 4, D–F
Top and bottom are expressed as fold of basal, and log EC_{50} is expressed as logged EC_{50} (M).

	$ZnCl_2$ (N = 3)	$NiCl_2$ (N = 3)	$NiSO_4$ (N = 3)
Top	2.19 ± 0.06	2.20 ± 0.08	2.58 ± 0.10
Bottom	1.00 ± 0.03	0.98 ± 0.04	1.00 ± 0.05
Log EC_{50}	−4.09 ± 0.05	−4.73 ± 0.07	−4.88 ± 0.08
Hill slope	3.23 ± 1.40	2.53 ± 0.67	3.46 ± 1.95

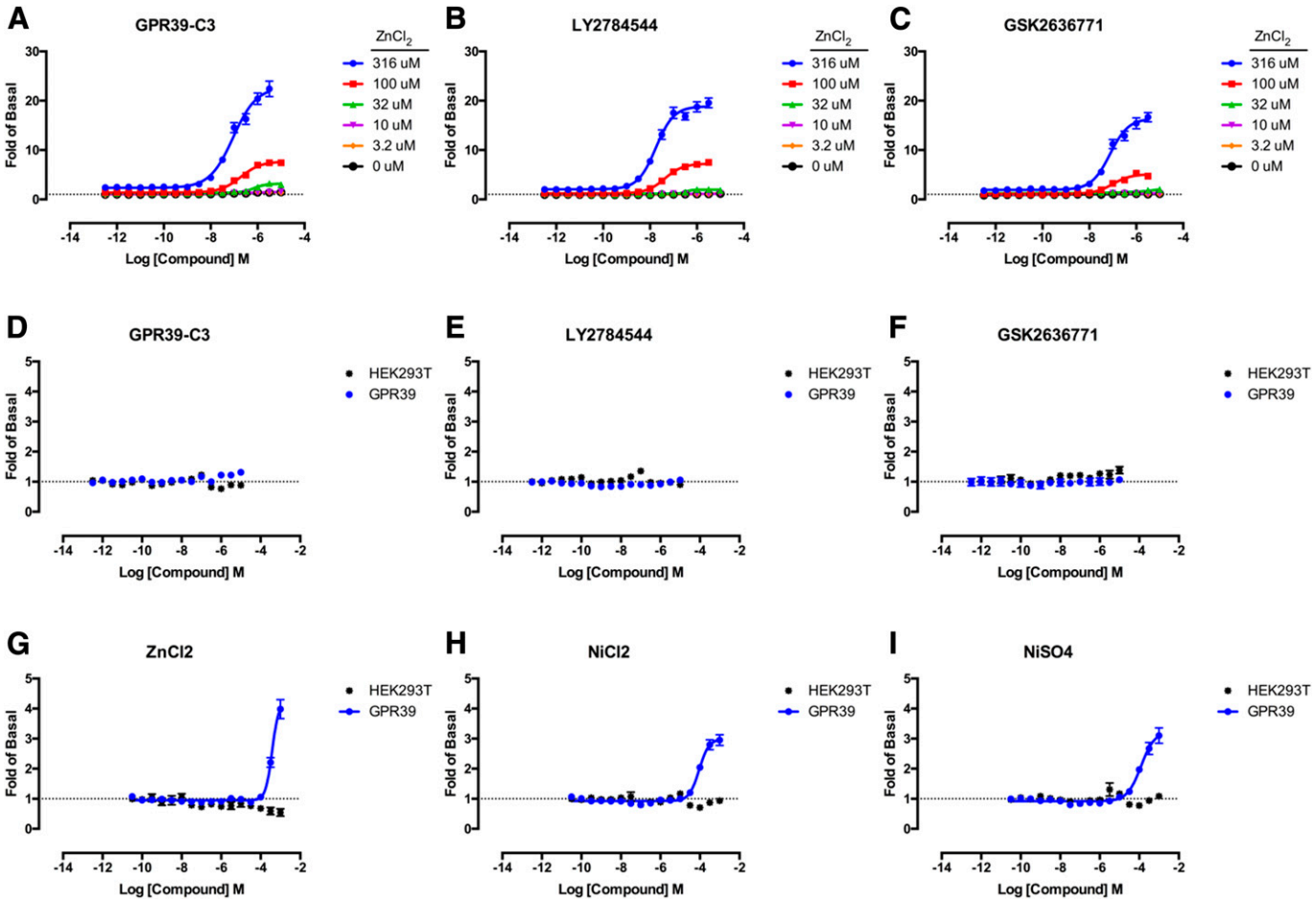

Fig. 5. Concentration-dependent and GPR39-dependent cAMP (Gs) responses, as measured by the Glosensor assay, to GPR39-C3 (A), LY2784544 (B), or GSK2636771 (C) with various concentrations of Zn^{2+}. Responses in the absence of Zn^{2+} are shown in (D), (E), and (F). Responses to $ZnCl_2$, $NiCl_2$, and $NiSO_4$ are shown in (G) and (H) and (I), respectively. The results are the mean ± S.E.M. of at least three independent experiments performed in quadruplicate.

results led to the conclusion that GPR39-C3, LY2784544, GSK2636771, Zn^{2+}, and Ni^{2+} can all act as agonists of GPR39-mediated Gq signaling, and that Zn^{2+} is a PAM of the responses of GPR39-C3, LY2784544 and GSK2636771.

Allosteric Modulation of GPR39 Gs-Mediated Signaling. In addition, we measured GPR39-mediated Gs pathway signaling (i.e., cAMP production) as described (see *Materials and Methods*). All three tested compounds, i.e., GPR39-C3,

TABLE 4
Pharmacological parameters of the results shown in Fig. 4, A–C
Top and bottom are expressed as fold of basal, and log EC_{50} is expressed as logged EC_{50} (M).

	$ZnCl_2$					
	316 μM (N = 3)	100 μM (N = 13)	31.6 μM (N = 3)	10 μM (N = 3)	3.16 μM (N = 3)	0 μM (N = 13)
GPR39-C3						
Top	22.76 ± 0.89	7.68 ± 0.15	3.18 ± 0.13	N.D.	N.D.	N.D.
Bottom	2.33 ± 0.24	1.38 ± 0.05	1.29 ± 0.04	N.D.	N.D.	N.D.
Log EC_{50}	−7.05 ± 0.07	−6.72 ± 0.04	−6.17 ± 0.08	N.D.	N.D.	N.D.
Hill slope	0.87 ± 0.10	1.01 ± 0.08	1.70 ± 0.45	N.D.	N.D.	N.D.
LY2784544						
Top	18.86 ± 0.38	7.24 ± 0.19	1.96 ± 0.07	N.D.	N.D.	N.D.
Bottom	2.04 ± 0.21	1.20 ± 0.10	1.12 ± 0.03	N.D.	N.D.	N.D.
Log EC_{50}	−7.75 ± 0.05	−7.37 ± 0.08	−6.47 ± 0.08	N.D.	N.D.	N.D.
Hill slope	1.14 ± 0.12	1.13 ± 0.37	3.31 ± 3.73	N.D.	N.D.	N.D.
GSK2636771						
Top	16.41 ± 0.51	4.80 ± 0.12	N.D.	N.D.	N.D.	N.D.
Bottom	1.93 ± 0.18	1.10 ± 0.05	N.D.	N.D.	N.D.	N.D.
Log EC_{50}	−7.12 ± 0.06	−7.09 ± 0.05	N.D.	N.D.	N.D.	N.D.
Hill slope	1.10 ± 0.14	1.29 ± 0.17	N.D.	N.D.	N.D.	N.D.

N.D., could not determine.

LY2784544, and GSK2636771, showed Zn^{2+}-dependent Gs signaling (Fig. 5, A–C; Table 4). Importantly, even GPR39-C3 showed a dramatic Zn^{2+} dependency of this response, despite not doing so in either β-arrestin recruitment (Fig. 3A) or Gq signaling (Fig. 4A). In untransfected cells, or in the absence of Zn^{2+}, neither of the compounds showed GPR39-mediated Gs pathway signaling (Fig. 5, D–F). At high concentrations, i.e., 30 μM and higher, Zn^{2+} and Ni^{2+} also acted as weak partial agonists of GPR39-mediated Gs pathway signaling (Fig. 5, G–I; Table 5). Thus, GPR39-C3, LY2784544, GSK2636771, Zn^{2+}, and Ni^{2+} can all act as agonists of GPR39-mediated Gs signaling, and additionally, Zn^{2+} is a PAM for the Gs-mediated responses of GPR39-C3, LY2784544, and GSK2636771.

Effects of Mutation of N-Terminal Histidine Residues on GPR39-Mediated Signaling. A previous study showed that mutation of two N-terminal histidine residues to alanine (H17A/H19A) in GPR39 led to a dysfunction in GPR39-mediated Gq signaling (Storjohann et al., 2008) such that Zn^{2+}-stimulated signaling was completely abolished. We wished to study the effects of these mutations further with respect to both various signaling pathways and various agonists and PAMs. First, using cell enzyme-linked immunosorbent assay, we established that the H17A/H19A double mutant of GPR39 was expressed similarly to the wild-type GPR39, both in the TANGO constructs as well as the "de-TANGO-ized" constructs (Supplemental Fig. 4). In Fig. 6 and Table 6, it can be seen that the H17A/H19A double mutant of GPR39 had little effect on β-arrestin recruitment activity in response to both the three small-molecule compounds of interest, as well as the activity of Zn^{2+} as a PAM of these responses. The double mutation completely abolished Gq signaling stimulated by either Zn^{2+} or Ni^{2+} (Fig. 7, D–F), consistent with the report by Storjohann et al. (2008). The double mutation had little or no effect on Gq signaling stimulated by GPR39-C3, LY2784544, or GSK2636771 in either the presence or absence of 100 μM Zn^{2+} (Fig. 7, A–C; Table 7). As with Gq signaling, the double mutation completely abolished Gs signaling stimulated by either Zn^{2+} or Ni^{2+} (Fig. 8, D–F). However, the double mutant showed reduced Gs signaling stimulated by GPR39-C3, LY2784544, or GSK2636771 with respect to both potency and efficacy (Fig. 8, A–C; Table 8).

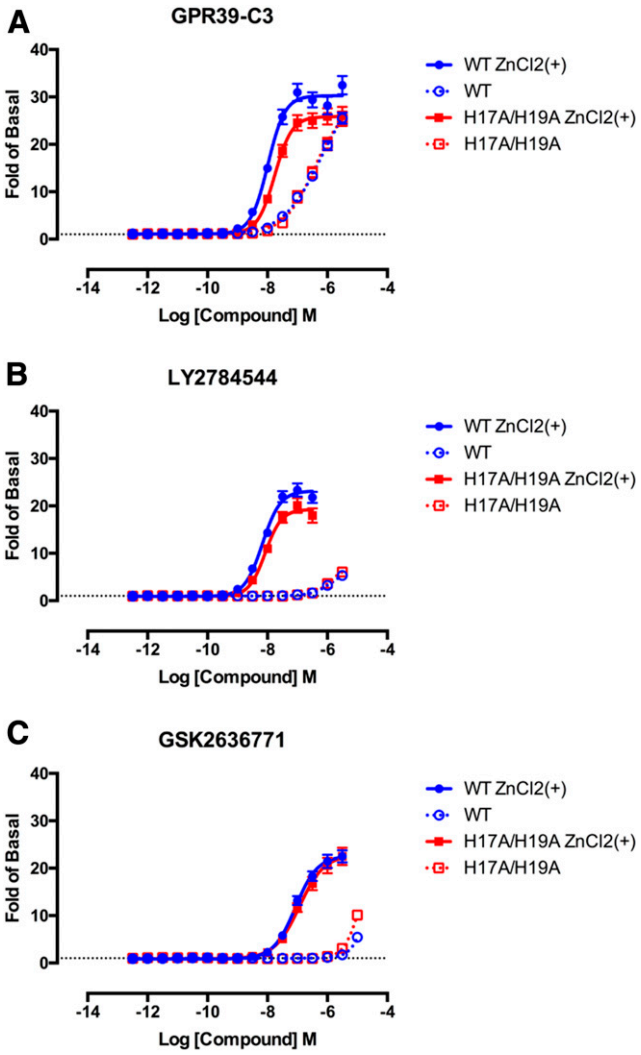

Fig. 6. Concentration-dependent β-arrestin recruitment responses of wild-type (WT) and H17A/H19A mutant receptors to GPR39-C3 (A), LY2784544 (B), and GSK2636771 (C) in the presence and absence of 100 μM Zn^{2+} as measured by the TANGO assay. The results are the mean ± S.E.M. of at least five independent experiments, each done in quadruplicate.

Discussion

Here, we report the discovery of novel GPR39 agonist scaffolds and the identification of zinc as a GPR39 PAM. These are the first results to identify zinc as a potent and frequently pathway- and probe-specific allosteric modulator for small-molecule GPR39 agonists. To discover these GPR39 agonists, we used a β-arrestin recruitment assay to screen several compound libraries comprising more than 5000 unique compounds for agonist activity at the orphan GPCR GPR39, which had previously been reported to be a divalent metal ion zinc receptor. Two compounds were found that had selective activity at GPR39—the JAK2 inhibitor LY2784544 and the PI3Kβ inhibitor GSK2636771 (Figs. 1 and 2). In additional studies, we showed that Zn^{2+} is an allosteric modulator of the responses of GPR39 to LY2784544 and GSK2636771, and that the allosteric actions of Zn^{2+} on these responses were stronger than for the selective GPR39 agonist, GPR39-C3 (Fig. 3). Currently, LY2784544 is being evaluated in patients with myeloproliferative neoplasm in two phase I trials to investigate dose and schedule (I3X-MC-JHTA, NCT01134120; and I3X-MC-JHTC, NCT01520220) and a phase II study to investigate efficacy (I3X-MC-JHTB, NCT01594723) (Ma et al., 2013). Additionally, GSK2636771 is being tested in a phase I/II trial in patients with phosphatase and tensin homolog (PTEN)–deficient advanced solid tumors (NCT01458067) (Thorpe et al., 2015). Indeed, when the potencies for activating GPR39 in the presence of Zn^{2+} were calculated, we found their EC_{50} values

TABLE 5

Pharmacological parameters of results shown in Fig. 5, G–I

The results are the mean ± S.E.M. of five independent experiments performed in quadruplicate. Top and bottom are expressed as fold of basal, and log EC_{50} is expressed as logged EC_{50} (M).

	$ZnCl_2$ (N = 7)	$NiCl_2$ (N = 5)	$NiSO_4$ (N = 5)
Top	4.22 ± 0.20	2.99 ± 0.07	3.24 ± 0.12
Bottom	0.95 ± 0.02	0.93 ± 0.02	0.92 ± 0.02
Log EC_{50}	−3.42 ± 0.04	−4.04 ± 0.04	−3.91 ± 0.06
Hill slope	2.62 ± 0.57	1.75 ± 0.24	1.25 ± 0.16

TABLE 6
Pharmacological parameters of results shown in Fig. 6
Top and bottom are expressed as fold of basal, and log EC_{50} is expressed as logged EC_{50} (M).

	WT		H17A/H19A	
	$ZnCl_2$ (+) (N = 8)	$ZnCl_2$ (−) (N = 8)	$ZnCl_2$ (+) (N = 5)	$ZnCl_2$ (−) (N = 5)
GPR39-C3				
Top	30.27 ± 0.57	33.25 ± 2.31	25.87 ± 0.55	29.07 ± 2.02
Bottom	1.09 ± 0.36	1.00 ± 0.16	1.08 ± 0.34	1.00 ± 0.24
Log EC_{50}	−7.99 ± 0.04	−6.22 ± 0.11	−7.76 ± 0.04	−6.43 ± 0.10
Hill slope	1.52 ± 0.17	0.69 ± 0.05	1.51 ± 0.18	0.84 ± 0.10
LY2784544				
Top	23.16 ± 0.52	7.10 ± 0.78	19.26 ± 0.56	7.23 ± 0.97
Bottom	0.89 ± 0.25	1.00 ± 0.03	0.91 ± 0.27	1.00 ± 0.06
Log EC_{50}	−8.17 ± 0.04	−5.81 ± 0.11	−8.07 ± 0.04	−5.91 ± 0.12
Hill slope	1.45 ± 0.15	1.27 ± 0.16	1.61 ± 0.23	1.57 ± 0.38
GSK2636771				
Top	22.61 ± 0.59	N.D.	22.85 ± 0.93	N.D.
Bottom	0.831 ± 0.21	1.00 ± 0.03	0.91 ± 0.27	1.00 ± 0.07
Log EC_{50}	−7.068 ± 0.04	>−4.00	−6.94 ± 0.06	>−4.00
Hill slope	1.179 ± 0.11	1.59 ± 0.86	1.05 ± 0.13	1.703 ± 0.75

N.D., could not determine; WT, wild type.

were in the sub- to single-digit nanomolar range in whole-cell assays. By comparison, the potency of LY2784544 in whole-cell assays for inhibition of JAK2 proliferation was 20 nM (Ma et al., 2013), whereas GSK2636771 had a potency of 7–114 nM in whole-cell assays (Qu et al., 2015). These results indicate that, in terms of the cellular context, the activities at GPR39 could predominate.

Given that these compounds are being tested in clinical trials, it should be of interest to establish whether they activate off-targets. Also, if side effects of these compounds are found, it may be possible to link the side effects to the off-targets rather than the targets and, thus, to provide clues as to the physiologic function(s) of orphan off-targets. In a clinical study of LY2784544, diarrhea, nausea, anemia, and transient increases in serum creatinine, uric acid, and potassium have been reported and attributed to a "typical tumor lysis syndrome" (Tefferi, 2012); however, it seems conceivable that at least some of these effects might be due to activation of GPR39. Interestingly, GPR39 is highly expressed in human colorectal adenocarcinoma HT-29 cells, and Zn^{2+} and a GPR39 agonist stimulated Gq signaling and promoted survival in these cells (Cohen et al., 2012, 2014; Boehm et al., 2013). By using the fluorescent imaging plate reader assay, we have shown that GPR39-C3, LY2784544, and GSK2636771 strongly activate the Gq pathway in HT-29 cells (Supplemental Fig. 5). Since LY2784544 shows modulator activity in the presence of physiologic concentrations of Zn^{2+}, it will be important to determine in clinical trials whether its side effects are due to its activity at GPR39.

Moreover, Zn^{2+} induced increased cell growth and survival in GPR39-expressing human prostate cancer PC-3 cells (Dubi et al., 2008; Asraf et al., 2014). Importantly, prostate tissue is rich in Zn^{2+} (Györkey et al., 1967; Zaichick et al., 1997). In the absence of Zn^{2+}, the selective PI3Kβ inhibitor GSK2636771

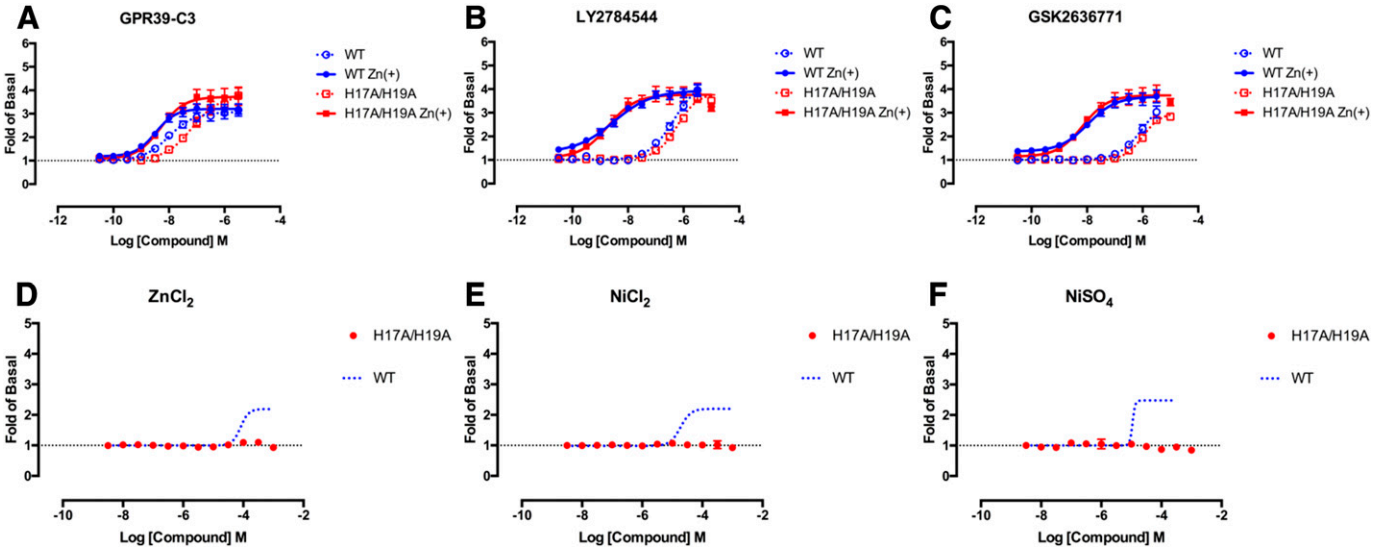

Fig. 7. Concentration-dependent phosphatidylinositol hydrolysis responses (Gq pathway) to GPR39-C3 (A), LY2784544 (B), and GSK2636771 (C) in the presence and absence of 100 μM Zn^{2+} at wild-type (WT) and H17A/H19A mutant receptors. Concentration-dependent PI hydrolysis responses (Gq pathway) to $ZnCl_2$ (D), $NiCl_2$ (E), or $NiSO_4$ (F). The results are the mean ± S.E.M. of at least three independent experiments, each done in quadruplicate.

TABLE 7
Pharmacological parameters of results shown in Fig. 7
Top and bottom are expressed as fold of basal, and log EC_{50} is expressed as logged EC_{50} (M).

	WT		H17A/H19A	
	$ZnCl_2$ (+) (N = 4)	$ZnCl_2$ (−) (N = 4)	$ZnCl_2$ (+) (N = 3)	$ZnCl_2$ (−) (N = 3)
GPR39-C3				
Top	3.21 ± 0.08	3.07 ± 0.10	3.72 ± 0.14	3.75 ± 0.22
Bottom	1.18 ± 0.11	1.00 ± 0.10	1.07 ± 0.17	1.03 ± 0.11
Log EC_{50}	−8.48 ± 0.10	−8.00 ± 0.12	−8.30 ± 0.14	−7.17 ± 0.14
Hill slope	1.20 ± 0.30	0.94 ± 0.23	1.01 ± 0.29	0.90 ± 0.23
LY2784544				
Top	3.94 ± 0.12	4.41 ± 0.38	3.77 ± 0.13	3.85 ± 0.16
Bottom	1.31 ± 0.22	1.00 ± 0.07	1.09 ± 0.27	1.03 ± 0.04
Log EC_{50}	−8.51 ± 0.16	−6.35 ± 0.14	−8.72 ± 0.18	−6.23 ± 0.07
Hill slope	0.63 ± 0.15	0.94 ± 0.18	0.88 ± 0.29	1.15 ± 0.15
GSK2636771				
Top	3.68 ± 0.12	3.68 ± 0.63	3.74 ± 0.12	3.00 ± 0.11
Bottom	1.36 ± 0.12	1.01 ± 0.05	1.14 ± 0.15	1.01 ± 0.02
Log EC_{50}	−7.97 ± 0.13	−5.99 ± 0.25	−8.16 ± 0.13	−5.99 ± 0.05
Hill slope	0.86 ± 0.20	1.01 ± 0.28	0.95 ± 0.24	1.35 ± 0.16

WT, wild type.

significantly decreases cell viability in p110β-reliant PTEN-deficient PC-3 cells (Weigelt et al., 2013). In the present study, we discovered that GSK2636771 could promote GPR39-selective intracellular signaling, which was markedly enhanced by the divalent metal ion Zn^{2+} (Figs. 3–5). Additionally, we have confirmed GPR39- and Gq-mediated Ca^{2+} release in PC-3 cells after stimulation with GPR39 agonists in the presence of Zn^{2+} (Supplemental Fig. 6). Since GSK2636771 has been developed as a potential treatment of PTEN-deficient advanced solid tumors, including colorectal cancer, it may be important to consider possible off-target effects of this compound due to its actions at GPR39. In addition, and more generally, our approach shows that new activities for compounds and new modulators for poorly annotated GPCRs can be discovered by screening modestly sized libraries of already-known small molecules.

The divalent metal ion Zn^{2+} has been reported to allosterically modulate GPCR function, not only GPR39 but also 5HT1A-serotonin (Barrondo and Sallés, 2009; Satała et al., 2015), α(1A)-adrenoreceptor (Ciolek et al., 2011), and β2-adrenergic receptor (Swaminath et al., 2002). Furthermore, the divalent metal ion Zn^{2+} can stimulate GPR68 (Abe-Ohya et al., 2015) and GPRC6A (Pi and Quarles, 2012; Pi et al., 2012) in the micromolar to millimolar range. Interestingly, Zn^{2+} modulates GPR39 activity via the Gq, Gs, and β-arrestin pathways (Holst et al., 2007). Other divalent cations, including Ni^{2+} (Holst et al., 2007) and even Cr^{2+}, Fe^{2+}, and Cd^{2+} (Huang et al., 2015), can also activate GPR39. In general, most GPCRs can modulate one G protein signaling pathway in addition to the β-arrestin pathway, although there are many exceptions. Our data show that LY2784544 and GSK2636771 can strongly stimulate Gq (Fig. 4), Gs (Fig. 5), and β-arrestin (Fig. 3) pathways. However, the mechanisms of stimulation of these compounds may not be the same and may not be shared with Zn^{2+} or GPR39-C3. For example, the Zn^{2+}-dependent enhancement of potency in the Gq and β-arrestin pathways induced by LY2784544 and

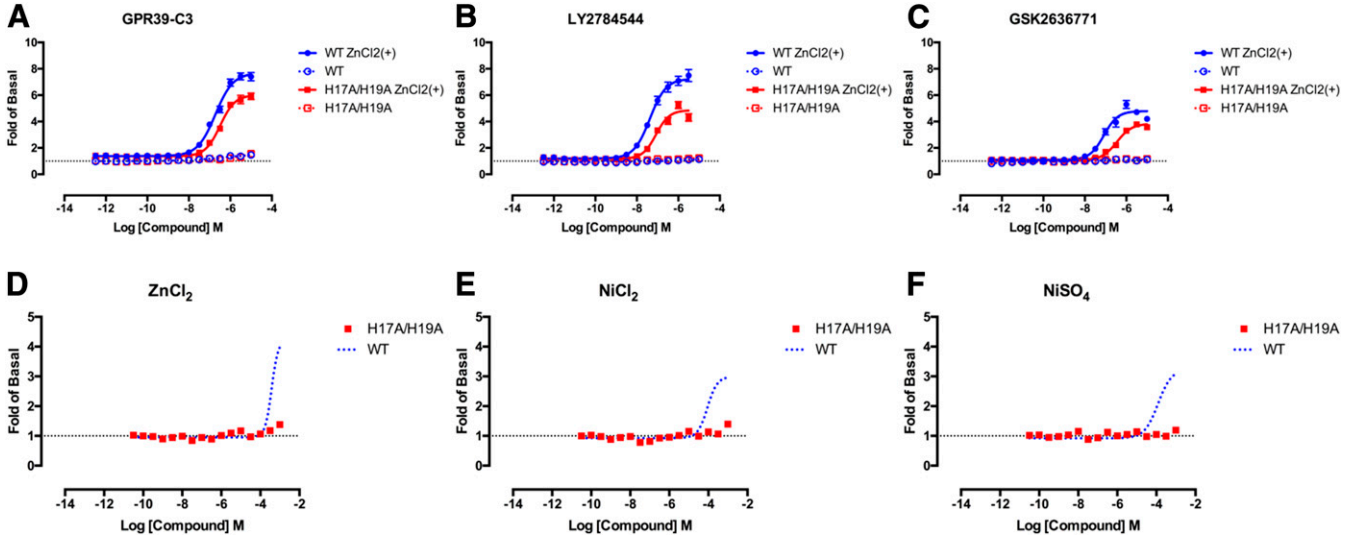

Fig. 8. Concentration-dependent cAMP production (Gs pathway) to GPR39-C3 (A), LY2784544 (B), and GSK2636771 (C) in the presence and absence of 100 μM Zn^{2+} at wild-type (WT) and H17A/H19A mutant receptors as measured by the Glosensor assay. Concentration-dependent cAMP production (Gs pathway) to $ZnCl_2$ (D), $NiCl_2$ (E), or $NiSO_4$ (F) at wild-type or H17A/H19A mutant receptors as measured by the Glosensor assay. The results are the mean ± S.E.M. of at least eight independent experiments, each in quadruplicate.

TABLE 8

Pharmacological parameters of the results shown in Fig. 8, A–C

The results are the mean ± S.E.M. of least eight independent experiments, each in quadruplicate. Top and bottom are expressed as fold of basal, and log EC_{50} is expressed as logged EC_{50} (M). The statistical significance of the difference in values between the wild type (WT) and mutant was determined using a one-sided *t* test.

	WT		H17A/H19A	
	$ZnCl_2$ (+) (N = 13)	$ZnCl_2$ (−) (N = 13)	$ZnCl_2$ (+) (N = 8)	$ZnCl_2$ (−) (N = 8)
GPR39-C3				
Top	7.68 ± 0.11	N.D.	6.01 ± 0.13*	N.D.
Bottom	1.38 ± 0.17	N.D.	1.37 ± 0.18	N.D.
Log EC_{50}	−6.72 ± 0.10	N.D.	−6.49 ± 0.12*	N.D.
Hill slope	1.01 ± 0.37	N.D.	1.22 ± 0.22	N.D.
LY2784544				
Top	7.24 ± 0.20	N.D.	4.86 ± 0.13*	N.D.
Bottom	1.20 ± 0.06	N.D.	1.17 ± 0.04	N.D.
Log EC_{50}	−7.37 ± 0.05	N.D.	−7.08 ± 0.05*	N.D.
Hill slope	1.13 ± 0.12	N.D.	1.35 ± 0.17	N.D.
GSK2636771				
Top	4.80 ± 0.12	N.D.	3.84 ± 0.12*	N.D.
Bottom	1.10 ± 0.05	N.D.	1.06 ± 0.03	N.D.
Log EC_{50}	−7.09 ± 0.05	N.D.	−6.46 ± 0.06*	N.D.
Hill slope	1.29 ± 0.17	N.D.	1.20 ± 0.16	N.D.

N.D., could not determine.
*$p < 0.05$.

GSK2636771, which have similar structures, is much greater than that induced by GPR39-C3 (Figs. 3 and 4), although clearly additional studies are needed to clarify the molecular details responsible for these intriguing signaling differences.

The potency and efficacy of Zn^{2+} alone in the β-arrestin pathway are quite small (Fig. 3). In the TANGO assay, which requires overnight incubation with ligand, the toxicity of high concentrations of Zn^{2+} prevented measurement of β-arrestin recruitment at these concentrations. However, it has been shown that Ni^{2+} can stimulate β-arrestin recruitment to GPR39 using a bioluminescence resonance energy transfer assay (Holst et al., 2007), and presumably, this would be similar to Zn^{2+}. In comparison with the activities of GPR39-C3, LY2784544, and GSK2636771, our results show that the responses to Zn^{2+} alone are quite small. We conclude that Zn^{2+} acts as a small-molecule PAM agonist at GPR39 for these two pathways.

Stimulation of the Gs (cAMP) pathway by compounds acting at GPR39 followed a very different pattern when compared with the Gq and β-arrestin pathways. The divalent cations Zn^{2+} and Ni^{2+} stimulated this pathway on their own; additionally, the GPR39-C3 compound, even without Zn^{2+}, showed significant Gs activity (Fig. 5). This is in agreement with a previous study (Peukert et al., 2014), which showed an EC_{50} value of 60 nM and an efficacy of 64% of the activity shown by 25 μM forskolin. Another study found that the GPR39 agonists AZ1395, 3,4-bis-(2-imidazol-1-ylethoxy)-benzonitrile; AZ4237, 6-[(4-chlorophenyl)methyl]-7-hydroxy-5-methyl-pyrazolo[1,5-a]pyrimidine-3-carboxylic acid; AZ7914, 6-(3-chloro-2-fluoro-benzoyl)-2-(2-methylthiazol-4-yl)-3,5,7,8-tetrahydropyrido-[4,3-d]pyrimidin-4-one also stimulated cAMP responses without Zn^{2+} (Fjellström et al., 2015); however, the phosphodiesterase inhibitor 3-isobutyl-1-methylxanthine (IBMX) was used in that study, which makes estimation of the "true" pharmacological parameters of these compounds difficult. Our results showed that all three compounds, i.e., GPR39-C3, LY2784544, and GSK2636771, had similar and significant Zn^{2+} dependency in their Gs responses, and were thus acting as PAM agonists with respect to Zn^{2+} in the Gs pathway.

The differences in the activities of the divalent cations and GPR39-C3, LY2784544, and GSK2636771 at GPR39 suggest that there may be multiple binding sites or modes for divalent cations in GPR39. It has already been shown that two histidine residues in the N terminus (H17 and H19) are involved in Zn^{2+} activity, since the Gq pathway response to concentrations of Zn^{2+} less than 1 mM is completely abolished by alanine substitution of these residues (Storjohann et al., 2008). Our results confirm these observations, and the response to Ni^{2+} was also abolished by these mutations (Fig. 7). Additionally, the Gs (cAMP) response to Zn^{2+} was also abolished by these mutations (Fig. 8). Thus, we conclude that H17 and H19 form one binding site for Zn^{2+} in GPR39. However, the H17A/H19A double mutation did not affect the activity of zinc or the zinc dependency of the activities of GPR39-C3, LY2784544, and GSK2636771 in the Gq or β-arrestin recruitment assays (Figs. 6 and 7). From this, we conclude that there must be an additional zinc-binding site in GPR39, that the zinc-binding sites act independently of each other, and that the H17/H19 zinc-binding site is orthosteric, whereas the yet-unknown additional site is allosteric.

In conclusion, here we report that the previously described "selective" kinase inhibitors LY2784544 and GSK2636771 have unexpectedly selective PAM agonist activity with respect to Zn^{2+} at GPR39. All tested compounds induced Gq, Gs, and β-arrestin signaling, and those responses are modulated by the divalent metal ion Zn^{2+} acting as a PAM agonist. We also clarified the roles of key residues in GPR39 relating only to divalent metal ion agonist activity by using mutagenesis. Although several ligands for GPR39 have been reported, whether there are endogenous ligands other than divalent metal ions for GPR39 is still not clear. Additionally, the physiologic functions of GPR39 signaling in vivo remain to be determined, and the scaffolds described here may provide starting points for novel chemical probes for GPR39.

Authorship Contributions

Participated in research design: Sato, Huang, Kroeze, Roth.
Conducted experiments: Sato, Huang, Kroeze.
Performed data analysis: Sato, Huang, Kroeze.
Wrote or contributed to the writing of the manuscript: Sato, Kroeze, Roth.

References

Abe-Ohya R, Ishikawa T, Shiozawa H, Suda K, and Nara F (2015) Identification of metals from osteoblastic ST-2 cell supernatants as novel OGR1 agonists. *J Recept Signal Transduct Res* **35**:485–492.

Asraf H, Salomon S, Nevo A, Sekler I, Mayer D, and Hershfinkel M (2014) The ZnR/GPR39 interacts with the CaSR to enhance signaling in prostate and salivary epithelia. *J Cell Physiol* **229**:868–877.

Assaf SY and Chung S-H (1984) Release of endogenous Zn^{2+} from brain tissue during activity. *Nature* **308**:734–736.

Barnea G, Strapps W, Herrada G, Berman Y, Ong J, Kloss B, Axel R, and Lee KJ (2008) The genetic design of signaling cascades to record receptor activation. *Proc Natl Acad Sci USA* **105**:64–69.

Barrondo S and Sallés J (2009) Allosteric modulation of 5-HT(1A) receptors by zinc: Binding studies. *Neuropharmacology* **56**:455–462.

Bhattacharyya S, Luan J, Farooqi IS, Keogh J, Montague C, Brennand J, Jorde L, Wareham NJ, and O'Rahilly S (2004) Studies of the neuromedin U-2 receptor gene in human obesity: evidence for the existence of two ancestral forms of the receptor. *J Endocrinol* **183**:115–120.

Bjarnadóttir TK, Gloriam DE, Hellstrand SH, Kristiansson H, Fredriksson R, and Schiöth HB (2006) Comprehensive repertoire and phylogenetic analysis of the G protein-coupled receptors in human and mouse. *Genomics* **88**:263–273.

Boehm M, Hepworth D, Loria PM, Norquay LD, Filipski KJ, Chin JE, Cameron KO, Brenner M, Bonnette P, Cabral S, et al. (2013) Chemical probe identification platform for orphan GPCRs using focused compound screening: GPR39 as a case example. *ACS Med Chem Lett* **4**:1079–1084.

Caroli S, Alimonti A, Coni E, Petrucci F, Senofonte O, and Violante N (1994) The Assessment of Reference Values for Elements in Human Biological Tissues and Fluids: A Systematic Review. *Crit Rev Anal Chem* **24**:363–398.

Ciolek J, Maïga A, Marcon E, Servent D, and Gilles N (2011) Pharmacological characterization of zinc and copper interaction with the human alpha(1A)-adrenoceptor. *Eur J Pharmacol* **655**:1–8.

Cohen L, Azriel-Tamir H, Arotsker N, Sekler I, and Hershfinkel M (2012) Zinc sensing receptor signaling, mediated by GPR39, reduces butyrate-induced cell death in HT29 colonocytes via upregulation of clusterin. *PLoS One* **7**: e35482.

Cohen L, Sekler I, and Hershfinkel M (2014) The zinc sensing receptor, ZnR/GPR39, controls proliferation and differentiation of colonocytes and thereby tight junction formation in the colon. *Cell Death Dis* **5**:e1307.

Dubi N, Gheber L, Fishman D, Sekler I, and Hershfinkel M (2008) Extracellular zinc and zinc-citrate, acting through a putative zinc-sensing receptor, regulate growth and survival of prostate cancer cells. *Carcinogenesis* **29**:1692–1700.

Feighner SD, Tan CP, McKee KK, Palyha OC, Hreniuk DL, Pong SS, Austin CP, Figueroa D, MacNeil D, Cascieri MA, et al. (1999) Receptor for motilin identified in the human gastrointestinal system. *Science* **284**:2184–2188.

Fjellström O, Larsson N, Yasuda S, Tsuchida T, Oguma T, Marley A, Wennberg-Huldt C, Hovdal D, Fukuda H, Yoneyama Y, et al. (2015) Novel Zn2+ Modulated GPR39 Receptor Agonists Do Not Drive Acute Insulin Secretion in Rodents. *PLoS One* **10**:e0145849.

Foster MC, Leapman RD, Li MX, and Atwater I (1993) Elemental composition of secretory granules in pancreatic islets of Langerhans. *Biophys J* **64**:525–532.

Frederickson CJ, Klitenick MA, Manton WI, and Kirkpatrick JB (1983) Cytoarchitectonic distribution of zinc in the hippocampus of man and the rat. *Brain Res* **273**:335–339.

Fredriksson R and Schiöth HB (2005) The repertoire of G-protein-coupled receptors in fully sequenced genomes. *Mol Pharmacol* **67**:1414–1425.

Györkey F, Min KW, Huff JA, and Györkey P (1967) Zinc and magnesium in human prostate gland: normal, hyperplastic, and neoplastic. *Cancer Res* **27**:1348–1353.

Holst B, Egerod KL, Jin C, Petersen PS, Østergaard MV, Hald J, Sprinkel AME, Størling J, Mandrup-Poulsen T, Holst JJ, et al. (2009) G protein-coupled receptor 39 deficiency is associated with pancreatic islet dysfunction. *Endocrinology* **150**: 2577–2585.

Holst B, Egerod KL, Schild E, Vickers SP, Cheetham S, Gerlach L-O, Storjohann L, Stidsen CE, Jones R, Beck-Sickinger AG, et al. (2007) GPR39 signaling is stimulated by zinc ions but not by obestatin. *Endocrinology* **148**:13–20.

Huang X-P, Karpiak J, Kroeze WK, Zhu H, Chen X, Moy SS, Saddoris KA, Nikolova VD, Farrell MS, Wang S, et al. (2015) Allosteric ligands for the pharmacologically dark receptors GPR68 and GPR65. *Nature* **527**:477–483.

Kenakin TP (2012) Biased signalling and allosteric machines: new vistas and challenges for drug discovery. *Br J Pharmacol* **165**:1659–1669.

Kojima M, Haruno R, Nakazato M, Date Y, Murakami N, Hanada R, Matsuo H, and Kangawa K (2000) Purification and identification of neuromedin U as an endogenous ligand for an orphan receptor GPR66 (FM3). *Biochem Biophys Res Commun* **276**:435–438.

Kojima M, Hosoda H, Date Y, Nakazato M, Matsuo H, and Kangawa K (1999) Ghrelin is a growth-hormone-releasing acylated peptide from stomach. *Nature* **402**: 656–660.

Komatsu H, Maruyama M, Yao S, Shinohara T, Sakuma K, Imaichi S, Chikatsu T, Kuniyeda K, Siu FK, Peng LS, et al. (2014) Anatomical transcriptome of G protein-coupled receptors leads to the identification of a novel therapeutic candidate GPR52 for psychiatric disorders. *PLoS One* **9**:e90134.

Kroeze WK, Sassano MF, Huang X-P, Lansu K, McCorvy JD, Giguère PM, Sciaky N, and Roth BL (2015) PRESTO-Tango as an open-source resource for interrogation of the druggable human GPCRome. *Nat Struct Mol Biol* **22**:362–369.

Lauwers E, Landuyt B, Arckens L, Schoofs L, and Luyten W (2006) Obestatin does not activate orphan G protein-coupled receptor GPR39. *Biochem Biophys Res Commun* **351**:21–25.

Lu J, Stewart AJ, Sleep D, Sadler PJ, Pinheiro TJT, and Blindauer CA (2012) A molecular mechanism for modulating plasma Zn speciation by fatty acids. *J Am Chem Soc* **134**:1454–1457.

Ma L, Clayton JR, Walgren RA, Zhao B, Evans RJ, Smith MC, Heinz-Taheny KM, Kreklau EL, Bloem L, Pitou C, et al. (2013) Discovery and characterization of LY2784544, a small-molecule tyrosine kinase inhibitor of JAK2V617F. *Blood Cancer J* **3**:e109.

Manglik A, Lin H, Aryal DK, McCorvy JD, Dengler D, Corder G, Levit A, Kling RC, Bernat V, Hübner H, et al. (2016) Structure-based discovery of opioid analgesics with reduced side effects. *Nature* **537**:185–190.

Młyniec K, Gaweł M, Librowski T, Reczyński W, Bystrowska B, and Holst B (2015a) Investigation of the GPR39 zinc receptor following inhibition of monoaminergic neurotransmission and potentialization of glutamatergic neurotransmission. *Brain Res Bull* **115**:23–29.

Młyniec K, Gaweł M, and Nowak G (2015b) Study of antidepressant drugs in GPR39 (zinc receptor$^{-/-}$) knockout mice, showing no effect of conventional antidepressants, but effectiveness of NMDA antagonists. *Behav Brain Res* **287**:135–138.

Młyniec K and Nowak G (2015) Up-regulation of the GPR39 Zn2+-sensing receptor and CREB/BDNF/TrkB pathway after chronic but not acute antidepressant treatment in the frontal cortex of zinc-deficient mice. *Pharmacol Rep* **67**:1135–1140.

Młyniec K, Singewald N, Holst B, and Nowak G (2015c) GPR39 Zn(2+)-sensing receptor: a new target in antidepressant development? *J Affect Disord* **174**:89–100.

Moran BM, Abdel-Wahab YH, Vasu S, Flatt PR, and McKillop AM (2016) GPR39 receptors and actions of trace metals on pancreatic beta cell function and glucose homoeostasis. *Acta Diabetol* **53**:279–293 Springer Milan.

Overington JP, Al-Lazikani B, and Hopkins AL (2006) How many drug targets are there? *Nat Rev Drug Discov* **5**:993–996.

Peukert S, Hughes R, Nunez J, He G, Yan Z, Jain R, Llamas L, Luchansky S, Carlson A, Liang G, et al. (2014) Discovery of 2-Pyridylpyrimidines as the First Orally Bioavailable GPR39 Agonists. *ACS Med Chem Lett* **5**:1114–1118.

Pi M and Quarles LD (2012) GPRC6A regulates prostate cancer progression. *Prostate* **72**:399–409.

Pi M, Wu Y, Lenchik NI, Gerling I, and Quarles LD (2012) GPRC6A mediates the effects of L-arginine on insulin secretion in mouse pancreatic islets. *Endocrinology* **153**:4608–4615.

Popovics P and Stewart AJ (2011) GPR39: a Zn(2+)-activated G protein-coupled receptor that regulates pancreatic, gastrointestinal and neuronal functions. *Cell Mol Life Sci* **68**:85–95.

Qu J, Rivero RA, Sanchez R, and Tedesco R (2015) inventors, GlaxoSmithKline, assignee. Benzimidazole derivatives as PI3 kinase inhibitors. U.S. patent 14/ 712,991. 2015 May 15.

Rask-Andersen M, Masuram S, and Schiöth HB (2014) The druggable genome: Evaluation of drug targets in clinical trials suggests major shifts in molecular class and indication. *Annu Rev Pharmacol Toxicol* **54**:9–26.

Regard JB, Sato IT, and Coughlin SR (2008) Anatomical profiling of G protein-coupled receptor expression. *Cell* **135**:561–571.

Roth BL and Kroeze WK (2015) Integrated Approaches for Genome-wide Interrogation of the Druggable Non-olfactory G Protein-coupled Receptor Superfamily. *J Biol Chem* **290**:19471–19477.

Satała G, Duszyńska B, Stachowicz K, Rafalo A, Pochwat B, Luckhart C, Albert PR, Daigle M, Tanaka KF, Hen R, et al.(2015) Concentration-dependent dual mode of Zn action at serotonin 5-HT1A receptors: in vitro and in vivo studies. *Mol Neurobiol* DOI: 10.1007/s12035-015-9586-3[published ahead of print].

Storjohann L, Holst B, and Schwartz TW (2008) Molecular mechanism of Zn2+ agonism in the extracellular domain of GPR39. *FEBS Lett* **582**:2583–2588.

Swaminath G, Steenhuis J, Kobilka B, and Lee TW (2002) Allosteric modulation of β2-adrenergic receptor by Zn(2+). *Mol Pharmacol* **61**:65–72.

Tanaka K, Masu M, and Nakanishi S (1990) Structure and functional expression of the cloned rat neurotensin receptor. *Neuron* **4**:847–854.

Tefferi A (2012) JAK inhibitors for myeloproliferative neoplasms: clarifying facts from myths. *Blood* **119**:2721–2730.

Thorpe LM, Yuzugullu H, and Zhao JJ (2015) PI3K in cancer: divergent roles of isoforms, modes of activation and therapeutic targeting. *Nat Rev Cancer* **15**:7–24.

Vassilatis DK, Hohmann JG, Zeng H, Li F, Ranchalis JE, Mortrud MT, Brown A, Rodriguez SS, Weller JR, Wright AC, et al. (2003) The G protein-coupled receptor repertoires of human and mouse. *Proc Natl Acad Sci USA* **100**:4903–4908.

Verhulst PJ, Lintermans A, Janssen S, Loeckx D, Himmelreich U, Buyse J, Tack J, and Depoortere I (2011) GPR39, a receptor of the ghrelin receptor family, plays a role in the regulation of glucose homeostasis in a mouse model of early onset diet-induced obesity. *J Neuroendocrinol* **23**:490–500.

Vita N, Oury-Donat F, Chalon P, Guillemot M, Kaghad M, Bachy A, Thurneyssen O, Garcia S, Poinot-Chazel C, Casellas P, et al. (1998) Neurotensin is an antagonist of the human neurotensin NT2 receptor expressed in Chinese hamster ovary cells. *Eur J Pharmacol* **360**:265–272.

Weigelt B, Warne PH, Lambros MB, Reis-Filho JS, and Downward J (2013) PI3K pathway dependencies in endometrioid endometrial cancer cell lines. *Clin Cancer Res* **19**:3533–3544.

Yasuda S, Miyazaki T, Munechika K, Yamashita M, Ikeda Y, and Kamizono A (2007) Isolation of Zn2+ as an endogenous agonist of GPR39 from fetal bovine serum. *J Recept Signal Transduct Res* **27**:235–246.

Zaichick VYe, Sviridova TV, and Zaichick SV (1997) Zinc in the human prostate gland: normal, hyperplastic and cancerous. *Int Urol Nephrol* **29**:565–574.

Zeng F, Wind N, McClenaghan C, Verkuyl JM, Watson RP, and Nash MS (2012) GPR39 is coupled to TMEM16A in intestinal fibroblast-like cells. *PLoS One* **7**:e47686.

Zhang JV, Klein C, Ren PG, Kass S, VerDonck L, Moechars D, and Hsueh AJW (2007) Response to Comment on "Obestatin, a peptide encoded by the ghrelin gene, opposes ghrelin's effects on food intake". *Science* **315**:766.

Zhang JV, Ren PG, Avsian-Kretchmer O, Luo CW, Rauch R, Klein C, and Hsueh AJ (2005) Obestatin, a peptide encoded by the ghrelin gene, opposes ghrelin's effects on food intake. *Science* **310**:996–999.

Address correspondence to: Bryan L. Roth, Genetic Medicine Building, Room 4072, 120 Mason Farm Road, Chapel Hill, NC 27599. E-mail: bryan_roth@med.unc.edu